Proceedings of the ASME 2010 3rd Joint US-European Fluids Engineering Summer Meeting and 8th International Conference on Nanochannels, Microchannels, and Minichannels
FEDSM-ICNMM2010
August 1-5, 2010, Montreal, Canada

FEDSM-ICNMM2010-30602

EXPERIMENTS ON THE STABILITY OF TAYLOR-COUETTE FLOW WITH DIFFERENT RADIAL TEMPERATURE GRADIENT

Dong Liu
Research Center for Aircraft Parts Technology(ReCAPT), Gyeongsang National University, Jinju, Gyengnam, 660-701, South Korea
School of Energy and Power Engineering Jiangsu University, Zhenjiang 212013, China
liudong@ujs.edu.cn

Hyoung-Bum Kim
School of Mechanical and Aerospace Engineering Gyeongsang National University, Jinju, Gyeongnam, 660-701, South Korea
kimhb@gnu.ac.kr

ABSTRACT

The effect of the temperature gradient and the presence of slits in the outer cylinders involved in creating a Taylor-Couette flow was investigated by measuring the velocity field inside the gap simultaneously. The slits were azimuthally located along the inner wall of outer cylinder and the number of slits was 18. The results showed that the buoyant force due to the temperature gradient clearly generated the helical flow when the rotating Reynolds number is small. For the plain model, the transition to turbulent Taylor vortex flow is not affected by the temperature gradient considered in this study. In addition, the transition process of 18-slit model was accelerated due to the slit wall. As the temperature gradient became larger, the critical Reynolds number of the transition process decreased.

Keywords: Taylor-Couette flow; Slit wall; DPIV; Negative temperature gradient; Positive temperature gradient

INTRODUCTION

The rotating flow in the annular gap between two concentric cylinders exhibits interesting flow instability phenomena when the difference of the angular velocities of the inner cylinder and outer cylinder increases above a certain critical Reynolds number. This flow is called a Taylor-Couette flow after the pioneering work by Taylor (1923). Since then, many researchers have studied the instability causing Taylor vortices. Different methods were given for solving this eigenvalue problem by Jones (1985), Wereley and Lueptow (1998), Rigopoulos and Sheridan *et al*. (2003), Marques and Lopez (2006). These studies have been performed under plain wall and isothermal conditions. A few works have been addressed on the flow transition process under non-isothermal conditions.

Lee *et al*. (2009) studied Taylor-Couette system with different numbers of slits in the outer cylinder by using Digital particle image velocimetry (DPIV) method. However, their study was limited to the isothermal conditions. The temperature of the two rotating cylinders need not remain the same in many engineering problems. Lepiller *et al*. (2008) studied the influence of radial temperature heating on the stability of the circular Couette flow, in their experiment, the Grashof number varied from -1000 to 1000, and they found that a radial temperature gradient destabilizes the Couette flow leading to a pattern of traveling helicoidal vortices occurring only near the bottom of the system. They also found that the size of the pattern increases as the rotation frequency of the cylinder is increased. Hayase *et al.* (1992) studied the flow and heat transfer in the space between two coaxial cylinders by using numerical calculation. Lee and Minkowycz (1989) studied heat transfer characteristics by using the naphthalene sublimation technique in the annular gap between two short concentric cylinders which had either two smooth walls or one smooth and one axially slit wall. This study yielded qualitative information regarding heat transfer but did not address the flow phenomena inside the annular gap.

Although many works focus on the Taylor-Couette flow and some of them consider the temperature gradient and wall shape effect, there is little work on the flow transition process considering the wall shape and various radial temperature

gradient effects at the same time. The present work explored the effect of different radial temperature gradient quantified by the Grashof number and the presence of slits on the transition process of a Taylor-Couette flow. Digital particle image velocimetry (DPIV) was used to measure the flow field inside the gap. This study can help not only to improve the performance of fluid machinery, but also to understand flow instability phenomena in a Taylor-Couette flow.

APPARATUS AND EXPERIMENTAL METHOD

The geometries of the experimental models used in this study are shown in Fig.1. The inner cylinder was made of aluminum pipe with black coating to prevent the reflection of a laser, which has an external radius r_i =33mm. The outer cylinder was made of acryl and had an inner radius r_o =40mm. One model was a plain model and the other model had 18 slits in the outer cylinder. The annular gap (d) between the cylinders was 7mm and the length of the cylinders(L) was 336mm. The radius ratio (r_i/r_o) and aspect ratio (L/d) were 0.825 and 48, respectively, following the studies of Cole (1976) and Wereley and Lueptow (1998). The depth of each slit was 5mm. The inner cylinder was rotated with a belt and pulley driven by a micro stepping motor having a resolution of 400,000 steps per revolution. This micro stepper motor was controlled through a computer, which allowed for the precise control of angular velocity (Ω) and the acceleration to the preset velocity. The outer cylinder was kept stationary.

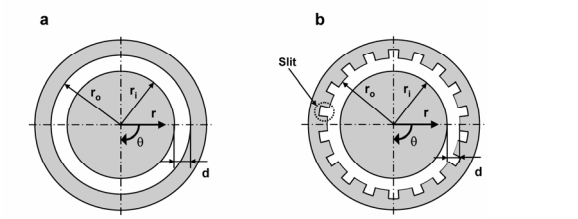

Fig. 1. Geometries of experimental models
(a) Plain model (b) 18-Slit model

Fig.2. shows the experimental apparatus and set-up to measure the velocity field. The working fluid sodium iodide solution filled the annular gaps and the space between the outer cylinder and the enclosure box in order to avoid the light refraction effect. The details of this method were explained in a previous study by Lee *et al*. (2009). To investigate the different temperature gradient effect, two heat exchangers were installed inside the inner cylinder and in the gap between the enclosure box and the outer cylinder, which were connected with constant temperature baths, and, by adjusting the temperature and the flow rate of constant temperature bath, different temperature gradient could be generated between two cylinders.

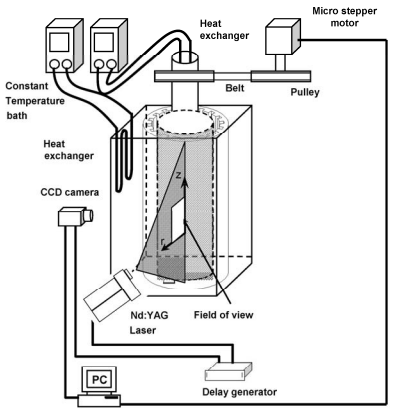

Fig.2. Schematic diagram of experimental apparatus

The effect of the temperature gradient is parameterized by the Grashof number, defined as $Gr = d^3 \beta g \Delta T / \nu$, where g is the acceleration due to gravity, β is the coefficient of the thermal expansion of the working fluid, and ΔT is the temperature change across the gap. ΔT is defined as ($T_i - T_o$) and is considered to be a negative temperature gradient if the inner cylinder is hotter than the outer cylinder. In this research, four different temperature gradients (ΔT), -6°C , -4°C, 4°C, and 6°C were used to study the effect on the flow transition process, and the Grashof number at each temperature gradient was -6700, -3600, 3600, and 6700, respectively. In this experiment, the rotational speed was expressed as a rotating Reynolds number, Re, which is defined as $Re=r_i d\Omega/\nu$, where Ω is the angular velocity of the inner cylinder.

EXPERIMENTAL RESULTS AND DISCUSSION

Radial and axial instantaneous velocity fields between the inner and outer cylinders were measured using the DPIV method. The axial position, Z*=z/d, and the radial position, $R^*=(r_o - r_i)/d$, were normalized by the annular gap width. Therefore, the latter (R*) varied from 0 at the wall of the inner cylinder to 1 at the wall of outer cylinder of a plain model. The region R*>1 refers to the axial slit space in the outer cylinder. Various flow regimes were classified quantitatively by measuring the velocity fields while increasing the Reynolds number.

Natural Convection Flow and Single Vortex Flow Regime

Due to the existence of the temperature gradient, a natural convection current was set up. The axial velocities (v_z) of both models under different Gr when the concentric cylinders were stationary (Re=0) are shown in Fig.3. From these results, we can find that negative temperature gradient created both an upward flow near the inner wall and a downward flow at the outer wall, which are the same results described by Deters and

Egbers (2005). For both models, we find that the axial velocity near the inner cylinder (R*=0) is larger than that near the outer cylinder (R*=1), and as the Gr increased from 3600 to 6700, the convection flow becomes stronger. That is, the axial velocity is increased. For the plain, the zero axial velocity is near the R*=0.5 location. However, the zero axial velocity of the 18-slit model moves to the outer cylinder, near the R*=0.7 location at both Gr. For the 18-slit model, the axial velocity near the slit wall is approximately 40% and 60% higher than the velocity near the inner cylinder when Gr is 3600 and 6700, respectively.

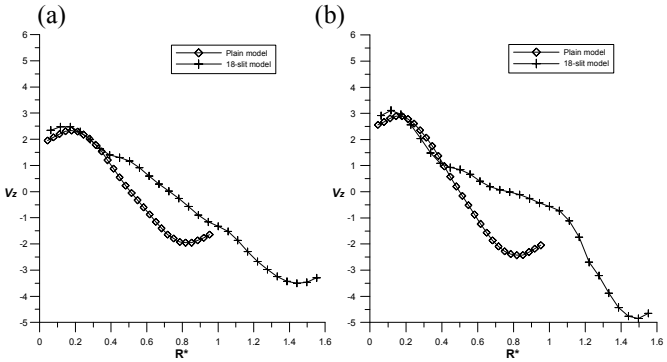

Fig. 3. Axial velocity profile by negative temperature gradient at Re=0
(a) Gr=3600 (b) Gr=6700

The convection flow in the plain model shows a nearly symmetrical shape. On the other hand, for 18-slit model, the flow rate near the outer cylinder is larger than that of the inner cylinder. From these results, we believe that the convection flow in the plain model is two-dimensional, but in the 18-slit model, the convection flow is three-dimensional with azimuthal velocity because the fluid flowed into the adjacent circumferential plane for mass balance.

As the Reynolds number gradually increased, the single vortex flow regime appeared in both negative and positive temperature gradient conditions. In this flow regime, only one counter-clockwise rotating vortex appeared at negative temperature gradient conditions and moved helically to the bottom of the cylinders, and a clockwise rotating vortex was found in positive temperature gradient conditions and moved to the top direction of the cylinders. This flow did not appear under isothermal conditions.

Helical Vortex Flow Regime

Fig.4. shows the critical Reynolds number of the transition from the single vortex flow regime to the helical vortex flow regime. In these two flow regimes, the vortices all moves helically along the axial direction. The differences between these two flow regimes are two counter-rotating vortices that appear in the helical vortex flow regime, unlike in the single vortex flow regime. By comparing the critical Reynolds number of different Gr and different models, we found the small slit number does not affect this transition process, which is the same as the results of the isothermal conditions described by Lee *et al*. (2009). From the plain model, this transition occurred at Re=80 when Gr was 3600, but for the 18-slit models of this Gr, this transition occurred a little earlier, at Re=71. As the Gr increased from 3600 to 6700, the transition accelerated in both models. Compared the results of the same value of $|Gr|$, the positive temperature gradient accelerates this transition process of all the models.

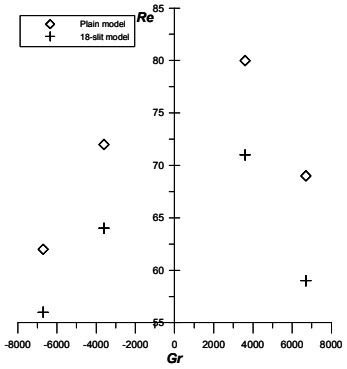

Fig. 4. Critical Reynolds number of the transition to helical vortex flow

Fig.5. shows the instantaneous flow fields of this flow regime at Re=99 at different temperature gradients. The background represents the vorticity distribution, which was calculated from the radial velocity v_r and axial velocity v_z using the equation $\omega = dv_r/dv_z - dv_z/dv_r$. Fig. 5a and b show the instantaneous velocity fields of the plain and 18-slit models when Gr is 3600; under this negative temperature gradient, the vortex pairs have the tendency to move to the bottom direction in both models. In Fig. 5c and d, the vortex pairs moved to the top direction, which was affected by the positive temperature gradient. Comparing the radial positions of the vortex centers in the vortex pair of the plain and 18-slit models, the vortex centers of each vortex nearly always have the same radial position in the plain model, while the center of the clockwise vortex in the vortex pairs is located closer to the inner cylinder under the negative temperature gradient and away from the inner cylinder under the positive temperature gradient in the 18-slit model. No obvious vortex was found in the slit space at this flow regime.

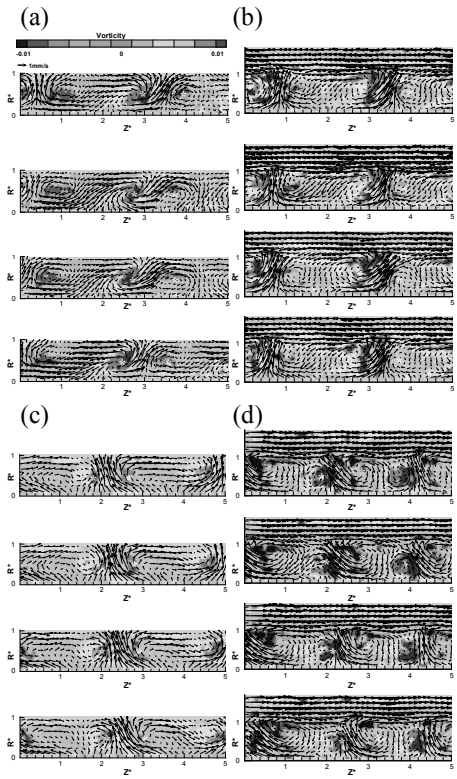

Fig. 5. Instantaneous velocity field of the helical vortex flow of at Re=99
(a) The plain model, Gr=3600 (b) The 18-slit, Gr=3600.
(c) The plain model, Gr=-3600 (d) The 18-slit, Gr=-3600

Helical Wavy Vortex Flow Regime

In plain model, the transition from helical vortex flow to helical wavy vortex flow occurred, but for the 18-slit model, this flow regime did not appear. Fig. 6. shows the critical Reynolds number of this transition process. As the Gr increased, this transition process occurred earlier . Under the same value of $|Gr|$, a positive temperature gradient accelerated this transition substantially.

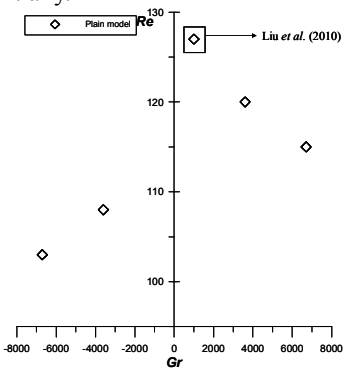

Fig. 6. Critical Reynolds number of the transition to helical wavy vortex flow

Fig.7. shows the instantaneous flow fields of this flow regime of the plain model at Re=130. At the same Reynolds number, a wavy vortex flow appeared under isothermal conditions (Lee et. al., 2009).

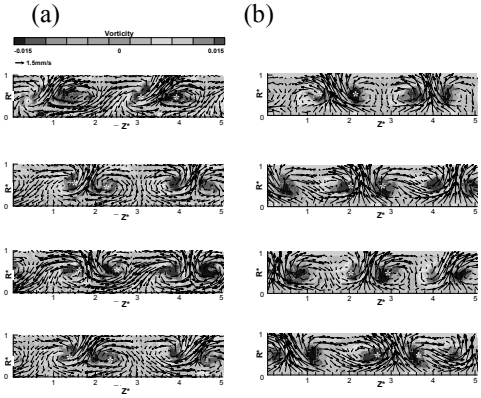

Fig. 7. Instantaneous velocity field of the helical wavy vortex flow of at Re=130
(a) Gr=3600. (b) Gr=3600.

Random Helical Vortex Flow Regime

With a further increase in the Reynolds number, the helical wavy flow changes into a random helical vortex flow, and critical Reynolds number of this transition process is shown in Fig. 8. In case of the 18-slit model, the transition to this flow regime is directly from the helical vortex flow. For the plain model, this transition occurred at Re=140. Larger and positive temperature gradients also accelerated the flow transition like other flow regime results. For the 18-slit model, the transition to the random helical vortex flow occurred at Re=128 when Gr is 3600, which is slightly more advanced than the result of a Gr of 1000 (Liu *et al*. 2010).

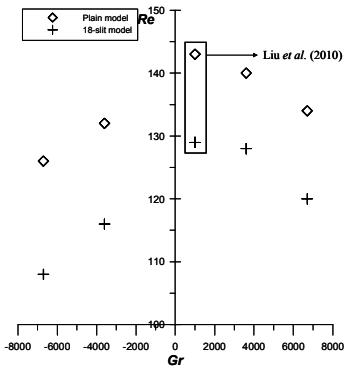

Fig.8. Critical Reynolds number of the transition to random helical vortex flow

Wavy Vortex Flow Regime

The wavy vortex flow regime only appeared in the plain model before the transition to a turbulent Taylor vortex flow. Fig.9. shows the critical Reynolds number of this transition process of the different models and temperature gradient. The

results show that the larger and positive temperature gradient accelerates the transition process.

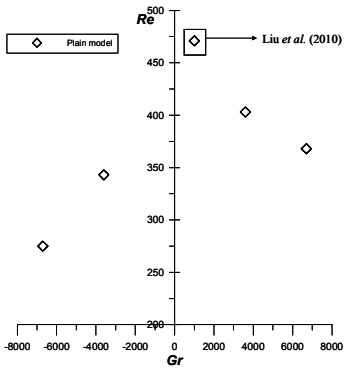

Fig.9. Critical Reynolds number of the transition to wavy vortex flow

The wavy frequency of the plain model at different Gr and different Re is shown in Fig.10. At the same $|Gr|$, the wavy frequency of wavy vortex flow under the negative temperature gradient effect is smaller, and as the temperature gradient increases, the wave frequency decreases.

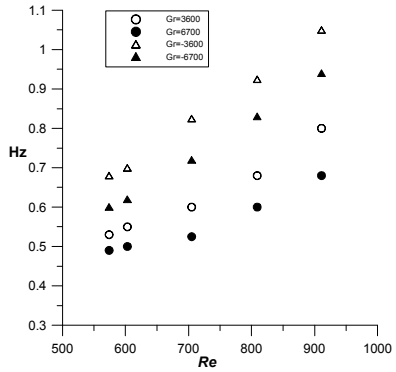

Fig. 10. Variation of the frequency of a wavy vortex in a plain model of different Gr

Turbulent Taylor Vortex Flow Regime

The flow of the plain model finally changed into a turbulent Taylor vortex flow as the rotating Reynolds number increased to 1909 under all the temperature gradient conditions, and this is identical to the isothermal conditions according to Lee *et al*. (2009). This means the temperature gradient considered in this study has no effect on the transition to turbulent Taylor vortex flow in these two models.

For the 18-slit model, it was found that the transition to a turbulent Taylor vortex flow was clearly accelerated compared to the plain model. Fig.11. shows the critical Reynolds number to a turbulent Taylor vortex flow of this model. As the temperature gradient increased, the turbulent Taylor vortex flow appeared earlier th 18-slit model.

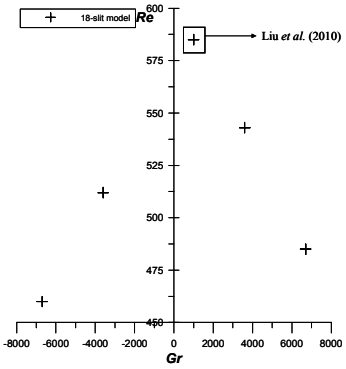

Fig. 11. Critical Reynolds number of the transition to turbulent Taylor vortex flow

CONCLUSION

An experimental study was performed for a Taylor-Couette flow with different temperature gradients between concentric cylinders with a slit wall. Through adjusting the rotation speed of the inner cylinder gradually, the effects of the temperature gradient and slit wall on the transition process from a laminar flow to a turbulent flow were investigated.

Before the inner cylinder starts to rotate, a natural convection flow was found in both plain and 18-slit models at both positive and negative temperature gradients. As the Re increased, a single vortex flow appeared. After this, a helical vortex flow, helical wavy vortex flow, random helical vortex, and wavy vortex flow appeared before the transition to turbulent Taylor vortex flow in the plain model. Positive or negative temperature gradients determine the direction of the rotation and movement of the vortex. For the 18-slit model, only the helical vortex flow and random helical vortex flow appeared before the transition to turbulent Taylor vortex flow. On the other hand, the 18-slit model accelerated all the transition processes. Comparing the results of different Gr, the positive and larger temperature gradients accelerate the transition process.

ACKNOWLEDGEMENT

This work was supported by the Priority Research Centers Program (2009-0094016) and the Pioneer Research Center Program (2009-0082813) through the National Research Foundation (NRF) of the Republic of Korea funded by the Ministry of Education, Science and Technology

REFERENCES

Cole J. A., 1976. Taylor-vortex instability and annulus-length effects. J. Fluid Mech. 75:1-15

Deters, T., Egbers, C., 2005, The Taylor-Couette system with radial temperature gradient, Journal of Physics: Conference Series, 138-142.

Lee, Y. N., Minkowycz, W. J., 1989, Heat transfer characteristics of the annulus of two-coaxial cylinders with one cylinder rotating, Int. J. Heat Mass Transfer, 32:711-722

Lee, S. H., Chung, H. T., Park, C. W., Kim, H. B., 2009, Experimental investigation of slit wall effects on Taylor-Couette flow. Fluid Dynamics Research. 41:1-12

Lepiller, V., Goharzadeh, A., Prigent, A., Mutabazi, I., 2008, Weak temperature gradient effect on the stability of the circular Couette flow, The European Physical Journal B, 61:445-455.

Liu D., Lee S. H., Kim H. B., 2010, Effect of a Constant Radial Temperature Gradient on a Taylor-Couette Flow with Axial Wall Slits. Fluid Dynamics Research.(submitted)

Marques, F., Lopez, J. M., 2006, Onset of three-dimensional unsteady states in small-aspect-ratio Taylor-Couette flow, J Fluid Mech, 561:255-277

Jones C. A., 1985, The transition to wavy Taylor vortices. J. Fluid Mech.157:135-62

Hayase T., J. Humphrey A. C., Greif R. 1992. Numerical calculation of convective heat transfer between rotating coaxial cylinders with periodically embedded cavities. J. Heat Trans. 114:589-597

Rigopoulos, J., Sheridan, J., Thompson, M. C., 2003, State selection in Taylor-vortex flow reached with an accelerated inner cylinder, J Fluid Mech, 489:79-99

Taylor G. I., 1923, Stability of a viscous liquid contained between two rotating cylinders, Phil Trans R Soc Lond, 223:289-343

Werely, S. T., Lueptow, R. M., 1998, Spatio-temporal character of non-wavy and wavy Taylor-Couette flow, J. Fluid Mech, 364:59-80